The integrals in Eqs. (A10) and (A12) were performed on an IBM-709 computer. The geometry discussed in Sec. III D with both 5° and 10° separation was used, and Ω was calculated as a function of E_8. The result is shown in Fig. 2.

An approximation based on Eq. (2) can be used to check the computer calculation for the case of very small detectors near the cone center. One introduces an effective cone solid angle Ω_c' as if the breakup were uniform over a cone of size Ω_c' with breakup probability

$$P(\alpha=0)=(1+\beta^2)/2\pi. \quad \text{(A13)}$$

Thus

$$\Omega_c'=1/P(0)=2\pi/(1+\beta^2), \quad \text{(A14)}$$

and

$$\Omega\approx\Omega_0^2(E_8+B)/(4\pi B). \quad \text{(A15)}$$

Equation (A15) was found to agree with the more exact computer calculation under the conditions described above.

PHYSICAL REVIEW VOLUME 138, NUMBER 6B 21 JUNE 1965

Low-Energy Elastic K^+-d Scattering with Separable Potentials*

J. H. HETHERINGTON AND L. H. SCHICK
School of Physics, University of Minnesota, Minneapolis, Minnesota

(Received 4 February 1965)

Low-energy K^+-d elastic-scattering cross sections are calculated using a Fadeev type of multiple-scattering formalism. The two-body interactions are taken to be S-wave nonlocal separable potentials of the Yamaguchi form. Coulomb forces, and the K^+-K^0 and n-p mass differences are neglected. The elastic angular distribution and cross section, as well as the total cross section, are calculated for incident kaon laboratory momenta in the range 110–230 MeV/c. In this momentum range it is found that for the elastic scattering cross sections the impulse-approximation result is within 10–25% and the double-scattering-approximation result is within 10% of the correct value. It is also found that in order for the optical theorem to give a good result for the total cross section, triple-scattering terms must be included. A detailed examination of the multiple-scattering series is made in order to illuminate these results.

I. INTRODUCTION

In a previous paper[1] a multiple-scattering formalism of the Fadeev type[2,3] for scattering from deuterons was derived and applied to low-energy K^--d scattering.[4] That particular application was chosen because the low-energy $\bar{K}$-N interactions were S-wave interactions and because some data on K^--d scattering was available. In fact the model for the $\bar{K}$-N interactions used in A did not completely justify using the results of the calculation to draw hard conclusions concerning experiment. As an investigation of the contribution of the single-scattering and the double-scattering terms to the exact solution of the multiple-scattering equations, however, these results were of interest. Even from this point of view the particular process studied was rather a special case in that the $\bar{K}$-N interactions are absorptive. The role played by unitarity was obscured by this absorption so that the scope of the interpretations which could be placed on the results was not clear.

In the present work we have applied the formalism developed in A to low-energy K^+-d scattering, a process in which the two-particle interactions are real. Partly because of our crude models for the two-particle interactions and partly because of the lack of data, our primary aim is not a comparison of our calculated results with experiment. Instead we shall concentrate on investigating the contributions of the low-order terms of the multiple-scattering series to the exact solution. Our aim is to see if there exist convenient approximations which may then be used in conjunction with more realistic two-particle interactions.

The model used here incorporates the same broad features as that used in A. Calculations are carried out for incident kaon laboratory momenta in the range 110–230 MeV/c. (For momenta $\gtrsim$300 MeV/c relativistic effects are large, while for momenta $\lesssim$100 MeV/c effects due to the K^+-K^0 and n-p mass differences become large. Neither relativistic nor mass-splitting effects are taken into account, although some calculations are done using relativistic kinematics.) Only S-wave interactions between pairs of particles are included. Each of the three interactions (K-N isospin

* Work supported by the U. S. Atomic Energy Commission.

[1] J. H. Hetherington and L. H. Schick, Phys. Rev. **137**, B935 (1965); hereafter referred to as A.

[2] L. D. Fadeev, Zh. Eksperim. i Teor. Fiz. **39**, 1459 (1960) [English transl.: Soviet Phys.—JETP **12**, 1014 (1961)]; Dokl. Akad. Nauk **138**, 561 (1961); **145**, 301 (1962) [English transls.: Soviet Phys.—Doklady **6**, 384 (1961); **7**, 600 (1963)].

[3] See also C. Lovelace, in *Strong Interactions in High Energy Physics*, edited by R. G. Moorhouse (Plenum Press, New York, 1964), p. 437; Phys. Rev. **136**, B1225 (1964).

[4] For similar developments of the n-d problem see A. N. Mitra and V. S. Bhasin, Phys. Rev. **131**, 1265 (1963); R. Aaron, R. D. Amado, and Y. Yam, *ibid.* **136**, B650 (1964); Phys. Rev. Letters **13**, 579 (1964).

singlet; K-N isospin triplet; and N-N isospin singlet, spin triplet) that enters the calculation is represented by a nonlocal separable potential of the Yamaguchi form.[5] Coulomb forces are neglected throughout, but the identity of the nucleons and intermediate charge-exchange scatterings are included.

In the next section we give the equations upon which the present calculations are based. In Sec. III we discuss the two-particle amplitudes which are used as input data. The results of the calculations of the elastic angular distribution, the elastic cross section, and the total cross section are given in Sec. IV. These cross sections are calculated in the impulse approximation,[6] the double-scattering approximation, and exactly for various values of the input parameters.[7] Since many features of the cross section can be related to the $l=0$ amplitude, which dominates the multiple-scattering corrections, Sec. V is devoted to a detailed examination of that amplitude and various approximations to it.

II. MULTIPLE-SCATTERING FORMALISM

The Schrödinger equation for the 3-body system is taken to be

$$\left\{\sum_{i=1}^{3}\frac{1}{2m_i}\nabla_i^2+\sum_{i=1}^{3}V_i\right\}\Psi=E\Psi, \tag{2.1}$$

where m_i is the mass of the ith particle, V_i is the potential-energy operator between particles j and k ($i\neq j$, $i\neq k$, $j\neq k$), and E is the total energy of the system. We let particle 2 be the kaon and particles 1 and 3 be the nucleons. All calculations are performed in the zero-total-momentum frame of reference.

Each two-body potential is taken to be an S-wave nonlocal separable potential for each isospin state and this latter quantum number is assumed to be conserved; i.e., in terms of isospin and configuration-space matrix elements

$$\langle\mathbf{r}_{jk};I|V_i|\mathbf{r}_{jk}';I'\rangle=\lambda_i(I)v_i(r_{jk};I)v_i(r_{jk}';I')\delta_{I,I'}, \tag{2.2}$$

where $\mathbf{r}_{jk}$ is the relative position vector of particles j and k, $r_{jk}=|\mathbf{r}_{jk}|$, and $I=I'$ is the total isospin of this pair of particles. We let $t_i(q,I)$ be the t-matrix operator for the scattering of particles j and k in their own center-of-mass system in a state of total isospin I and energy

$$E-\{(2m_i)^{-1}+(2\mathfrak{M}_i)^{-1}\}q^2, \tag{2.3}$$

where

$$\mathfrak{M}_i=m_j+m_k. \tag{2.4}$$

It follows from Eq. (2.2) that the (in general, off-energy-shell) matrix element of this operator for the scattering of particles j and k from a state of relative momentum $\mathbf{k}_i'$ to a state of relative momentum $\mathbf{k}_i$ is given by

$$\langle\mathbf{k}_i|t_i(q,I)|\mathbf{k}_i'\rangle=v_i(k_i,I)\tau_i(q,I)v_i(k_i',I), \tag{2.5}$$

where

$$v_i(k_i,I)=\int d\mathbf{r}_{jk}v_i(r_{jk};I)\exp[i\mathbf{k}_i\cdot\mathbf{r}_{jk}], \tag{2.6}$$

$$\tau_i(q,I)=\lambda_i(I)[1-\lambda_i(I)\gamma_i(q,I)]^{-1}, \tag{2.7}$$

$$\gamma_i(q,I)=\int\frac{d\mathbf{k}_iv_i^2(k_i,I)}{(2\pi)^3[E-(\mathfrak{M}/2m_i\mathfrak{M}_i)q^2-(k_i^2/2\mu_i)+i\eta]}, \tag{2.8}$$

$$\mathfrak{M}=m_1+m_2+m_3,\quad \mu_i=\mathfrak{M}_i^{-1}m_jm_k,\quad \eta\to 0^+. \tag{2.9}$$

The potential shapes are taken to be

$$v_i(k_i,I)=[k_i^2+\beta_i^2(I)]^{-1}. \tag{2.10}$$

The potential strengths $\lambda_i(I)$ and range parameters $\beta_i^{-1}(I)$ are to be determined from two-body experiments.

The elastic angular distribution, elastic cross section, and total cross section may be written in the form

$$(d\sigma_{\mathrm{EL}}/d\Omega)=(\mu_{Kd}/2\pi)^2|\sum(2l+1)\eta_lP_l(\hat{q}_a\cdot\hat{q}_b)|^2, \tag{2.11}$$

$$\sigma_{\mathrm{EL}}=(\mu_{Kd}^2/\pi)\sum(2l+1)|\eta_l|^2, \tag{2.12}$$

$$\sigma_{\mathrm{TOT}}=-(2\mu_{Kd}/q_a)\sum(2l+1)\,\mathrm{Im}(\eta_l). \tag{2.13}$$

Here $\mathbf{q}_a$ and $\mathbf{q}_b$ are the relative K^+-d momenta in the final and initial states, respectively, $\hat{q}_a=\mathbf{q}_a|\mathbf{q}_a|^{-1}$, $\hat{q}_b=\mathbf{q}_b|\mathbf{q}_b|^{-1}$, $q_a=|\mathbf{q}_a|=|\mathbf{q}_b|$, μ_{Kd} is the K^+-d reduced mass, P_l is the lth order Legendre polynomial, and η_l is the center-of-mass t-matrix element for elastic K^+-d scattering in the lth relative angular-momentum channel.

The isospin considerations, as well as the potential shapes, in this problem are the same as those that were used in A. Taking over the expression for η_l obtained there, we have

$$\eta_l=\eta_l^{\mathrm{IA}}+\eta_l^{\mathrm{MS}}, \tag{2.14}$$

$$\eta_l^{\mathrm{IA}}=\sum_{\gamma=1}^{3}\int_0^\infty\Phi_{l\gamma2}(q,q_a)\tau^\gamma(q)\Phi_{l\gamma2}(q,q_a)(2\pi)^{-2}q^2dq, \tag{2.15}$$

$$\eta_l^{\mathrm{MS}}=\sum_{\alpha=1}^{3}\sum_{\beta=1}^{3}\int_0^\infty\int_0^\infty\Phi_{l\alpha2}(q,q_a)\tau^\alpha(q)R_{l\alpha\beta}(q,q')\tau^\beta(q')\times\Phi_{l\beta2}(q',q_a)(2\pi)^{-4}q^2q'^2dqdq'. \tag{2.16}$$

Here η_l^{IA} is the single-scattering term in the multiple-scattering series for η_l, while η_l^{MS} is the contribution of all the higher order terms in this series.

The matrix element $R_{l\alpha\beta}(q,q')$ is given by the integral

[5] Y. Yamaguchi, Phys. Rev. **95**, 1628 (1954).

[6] In this paper the impulse approximation is taken to mean the first term of the multiple-scattering series as given in Eq. (2.15). This differs from the form used by Chew (see Ref. 16) discussed in Sec. V.

[7] For impulse-approximation treatments of K^+-d scattering see E. M. Ferreira, Phys. Rev. **115**, 1727 (1959); M. Gourdin and A. Martin, Nuovo Cimento **11**, 670 (1959); and Ref. 10 below.

equation

$$R_{l\alpha\beta}(q,q')=K_{l\alpha\beta}(q,q')+\sum_{\gamma=1}^{3}\int_0^\infty K_{l\alpha\gamma}(q,q'')\times\tau^\gamma(q'')R_{l\gamma\beta}(q'',q')(2\pi)^{-2}(q'')^2dq'', \quad (2.17)$$

where

$$K_{l\alpha\beta}(q,q')=\mathcal{Q}_l(Z_{\alpha\beta}(q,q'),Z_{\beta\alpha}(q',q),Z_{\alpha\beta}(E,q,q'))\times\frac{\mathfrak{M}_\alpha\mathfrak{M}_\beta m_0 W_{\alpha\beta}}{4m_\alpha m_\beta(qq')^3}, \quad (2.18)$$

with

$$\mathcal{Q}_l(Z_1,Z_2,Z_3)=\int_{-1}^{1}[(Z_1-\mu)(Z_2-\mu)(Z_3-\mu)]^{-1}\times P_l(\mu)d\mu, \quad (2.19)$$

$$Z_{\alpha\beta}(q,q')=-\frac{\mathfrak{M}_\alpha\beta_\alpha^2}{2m_\beta qq'}-\frac{\mathfrak{M}_\alpha q'}{2m_\beta q}-\frac{m_\beta q}{2\mathfrak{M}_\alpha q'}, \quad (2.20)$$

$$Z_{\alpha\beta}(E,q,q')=\frac{E^+m_0}{qq'}-\frac{\mathfrak{M}_\beta q}{2m_\alpha q'}-\frac{\mathfrak{M}_\alpha q'}{2m_\beta q}, \quad (2.21)$$

$$E^+=E+i\eta, \quad m_0=\mathfrak{M}-m_\alpha-m_\beta. \quad (2.22)$$

The isospin-space matrix $[W_{\alpha\beta}]$ has the form

$$[W_{\alpha\beta}]=\begin{bmatrix}-1/2 & 1/\sqrt{2} & \sqrt{3}/2\\ 1/\sqrt{2} & 0 & \sqrt{(3/2)}\\ \sqrt{3}/2 & \sqrt{(3/2)} & 1/2\end{bmatrix}, \quad (2.23)$$

while the "vector" $[\tau^\gamma(q)]$ is given by

$$[\tau^\gamma(q)]=\begin{bmatrix}\tau_1(q,0)\\ \tau_2(q,0)\\ \tau_1(q,1)\end{bmatrix}. \quad (2.24)$$

The $\tau_i(q,I)$ in this last expression are given in Eq. (2.7) where the subscript $i=2$ refers to the nucleon-nucleon interaction and the subscript $i=1$ refers to the K-N interaction. Expressions for the double-scattering, triple-scattering, and higher order multiple-scattering terms may be obtained by iteration of Eq. (2.17) and substitution of the result into Eq. (2.16).

Each factor $\Phi_{l\gamma 2}(q,q_a)$ appearing in Eqs. (2.15) and (2.16) is a component of the vector $[C_\gamma]$ times the lth partial-wave part of the product of the deuteron momentum-space wave function $\phi(|\mathbf{q}+(m_\gamma|\mathfrak{M}_2)\mathbf{q}_a|)$ and the potential shape $v_\gamma(|\mathbf{q}_a+(m_2|\mathfrak{M}_\gamma)\mathbf{q}|)$:

$$\Phi_{l\gamma 2}(q,q_\alpha)=-\mathcal{Q}_l(Z_{\gamma 2}(q,q_a),Z_{2\gamma}(q_a,q),\bar{Z}_{2\gamma}(q_a,q))\times\frac{\mathfrak{M}_2^2\mathfrak{M}_\gamma N_2 C_\gamma}{8m_2 m_\gamma^2(qq_a)^3}, \quad (2.25)$$

where

$$\bar{Z}_{2\gamma}=Z_{2\gamma} \quad \text{with} \quad \beta_2\rightarrow\alpha_2, \quad (2.26)$$

$$\alpha_2=(2\mu_2 B_2)^{1/2}, \quad B_2=2.225 \text{ MeV}, \quad (2.27)$$

$$N_2=8\pi\alpha_2\beta_2(\alpha_2+\beta_2)^3, \quad (2.28)$$

$$[C_\gamma]=\begin{bmatrix}1/2\\ 0\\ \sqrt{3}/2\end{bmatrix}. \quad (2.29)$$

Once the two-particle interactions given by Eqs. (2.7)–(2.10) are determined, Eqs. (2.14)–(2.29) may be used to evaluate the cross sections given in Eqs. (2.11), (2.22), and (2.13). We turn then to consider the two-particle amplitudes.

III. TWO-PARTICLE AMPLITUDE

The two-particle S-wave scattering amplitude $f_i(k,I)$ is related to the t-matrix element given in Eq. (2.5) by

$$f_i(k,I)=-(2\pi)^{-1}\mu_i\langle\mathbf{k}_i|t_i(q,I)|\mathbf{k}_i'\rangle, \quad (3.1)$$

with

$$k\equiv\{2\mu_i[E-(\mathfrak{M}q^2/2m_i\mathfrak{M}_i)]\}^{1/2}, \quad (3.2)$$

and the on-energy-shell condition $|\mathbf{k}_i|-|\mathbf{k}_i'|=k$. In terms of the S-wave phase shift $\delta_i(k,I)$

$$f_i(k,I)=[k\cot\delta_i(k,I)-ik]^{-1}. \quad (3.3)$$

It follows from these relations and Eqs. (2.7)–(2.10) that the phase shift corresponding to the two-body potential of Eq. (2.2) may be written

$$k\cot\delta_i(k,I)=a_i^{-1}(I)+\tfrac{1}{2}r_{0i}(I)k^2+P_i(I)k^4, \quad (3.4)$$

where the scattering length $a_i(I)$, the effective range $r_{0i}(I)$, and the shape parameter $P_i(I)$ are given by

$$a_i(I)=-\frac{2}{\beta_i(I)}\left[1+\frac{4\pi\beta_i^3(I)}{\mu_i\lambda_i(I)}\right]^{-1}, \quad (3.5)$$

$$r_{0i}(I)=\frac{1}{\beta_i(I)}\left[1-\frac{8\pi\beta_i^3(I)}{\mu_i\lambda_i(I)}\right], \quad (3.6)$$

$$P_i(I)=-2\pi[\mu_i\lambda_i(I)]^{-1}. \quad (3.7)$$

For the nucleon-nucleon interaction ($i=2$, $I=0$) only the ${}^3S_1$ potential enters the calculation. We have taken the values of the parameters for this potential that fit the low-energy data directly from Ref. 5. These values are

$$\alpha_2=45.706 \text{ MeV}/c, \quad \beta_2\equiv\beta_2(0)=6.255\alpha_2 \quad (3.8)$$

with

$$\lambda_2\equiv\lambda_2(0)=-8\pi\beta_2(\alpha_2+\beta_2)^2 m_1^{-1}. \quad (3.9)$$

The determination of the kaon-nucleon potential parameters is not so straightforward.

We consider first the K-N isospin triplet interaction. The analysis of Goldhaber *et al.*[8] showed that for kaon lab momenta up to 640 MeV/c, K^+-p scattering is pure S-wave scattering. The data could be fit by both a purely repulsive hard-core potential with a radius of 0.31 F and an effective-range model,

$$k\cot\delta_1=a_1^{-1}+\tfrac{1}{2}r_{01}k^2, \quad (3.10)$$

[8] S. Goldhaber *et al.*, Phys. Rev. Letters **9**, 135 (1962).

with

$$a_1=(-0.29\pm0.015)\text{ F},\quad r_{01}=(0.5\pm0.15)\text{ F}. \tag{3.11}$$

With our model, on the other hand, Eqs. (3.5) and (3.6) yield

$$\beta_1\equiv\beta_1(1)=(3/2r_{01})\{1\pm[1+16r_{01}/9a_1]^{1/2}\}, \tag{3.12}$$

$$\lambda_1\equiv\lambda_1(1)=-(4\pi\beta_1{}^3/\mu_1)[2/\beta_1a_1+1]^{-1}. \tag{3.13}$$

For a negative scattering length the requirement that the right-hand side of Eq. (3.12) be real leads to the inequality

$$(r_{01}/|a_1|)<(9/16). \tag{3.14}$$

This inequality is not satisfied by the values of r_{01} and a_1 given in Eq. (3.11).

The failure of our model to reproduce the experimental scattering length and effective range is not particular to the shape of $v_i(k,1)$ used here. The difficulty lies in the fact that the negative scattering length and relatively large effective range require a local potential which changes sign; i.e., a potential which if strongly repulsive at small distances is weakly attracitve at larger distances. It is well known that a *sum* of nonlocal separable potentials is required to duplicate the physical properties of such a local potential. Since our model can be made a very good fit to the experimental data at lower energies, we did not feel it was worthwhile to include such sums of separable potentials at this time. We have therefore continued to use the single separable potential with the shape $v_1(k,1)$ as given above.

Fortunately, for the momentum region of interest we may adjust the parameters of our K-N potential in such a manner as to obtain good agreement with the K^+-p experimental results while at the same time insuring that the discrepancy between these values of the parameters and those given in Eq. (3.11) does not distort the results of the present calculation. We see from Eqs. (3.4) and (3.7) that we may make our model independent of the shape parameter by choosing λ_1 suitably large. By choosing $a_1=-0.29$ F we have, for values of $k\approx0$, agreement with the K^+-p experimental result. Further, we maintain this agreement for values of $k\lesssim300$ MeV/c so long as we choose an $r_{01}\lesssim0.5$ F; i.e., so long as our r_{01} is small enough that in this momentum range the first term on the right-hand side of Eq. (3.10) dominates. Equation (3.14) guarantees that for $a_1=-0.29$ F this is the case.

To insure a sufficiently large value of λ_1 we chose

$$[2(\beta_1|a_1|)^{-1}-1]=0.001. \tag{3.15}$$

This relation along with the experimental value for a_1 then gave us

$$\beta_1{}^{-1}=0.145145\text{ F},\quad r_{01}=0.145\text{ F}. \tag{3.16}$$

Preliminary calculations of the various K^+-d cross sections showed that λ_1 could be varied by a factor of 10 from the value determined by Eqs. (3.13), (3.15), and (3.16) without affecting the results at all.

Finally we note that it is only in the low-energy range in which our potential model fits experiment that the K-N t-matrix elements are evaluated in the multiple-scattering calculation. In Eqs. (2.15) and (2.16) the t-matrix elements have been decomposed as in Eq. (2.5). Only the factor $\tau^\gamma(q)$ appears explicitly, the potential shape factors having been absorbed into the $\Phi_{l\gamma2}(q,q_a)$ or $R_{l\alpha\beta}(q,q')$. For any range parameter $\beta_1{}^{-1}$ that is smaller than $\beta_2{}^{-1}$, the range parameter of the N-N potential, the structure of $\Phi_{l\gamma2}(q,q_a)$ is dominated by the deuteron wave function; i.e., the singularities of $\Phi_{l\gamma2}(q,q_a)$ in the q plane that lie closest to the real axis are the branch points characterized by the size of the deuteron $\alpha_2{}^{-1}$ and the range of the N-N potential. The closest singularity, the $\alpha_2{}^{-1}$ branch point, causes $\Phi_{l\gamma2}(q,q_a)$ to peak in the region $q\approx q_a/2$; i.e., $\bar{Z}_{2\gamma}=\pm1$ implies $\mathrm{Re}(q)=q_a/2$. The $\Phi_{l\gamma2}(q,q_a)$, as can be seen from Eqs. (2.19) and (2.20), fall off rapidly for both large and small q. Actual calculational experience shows that only values of $q\lesssim500$ MeV/c contribute significantly to the integrals in Eqs. (2.15) and (2.16). For such values of q Eq. (3.2) yields values for k^2 small enough for the K-N isotriplet amplitude to be dominated by the scattering length. A similar argument holds for the K-N isosinglet amplitude.

The K-N isosinglet data is quite meager for kaon lab momenta $\lesssim300$ MeV/c. There is evidence[9,10] that for momenta $\gtrsim300$ MeV/c this interaction includes a P-wave (and possibly a D-wave) component. We are concerned with momenta which are on the whole somewhat lower than this. We assume only an S-wave interaction. From K^+-d experiments Stenger *et al.*[10] estimated the isospin singlet S-wave scattering length to be

$$a_0\equiv a_1(0)=(0.04\pm0.04)\text{ F}. \tag{3.17}$$

Again in the momentum region of interest here the K-N $I=0$ scattering amplitude is dominated by the contribution from the scattering length and is not sensitive to the value of the effective range provided this range is small enough. We have chosen the effective range by arbitrarily setting

$$\beta_0{}^{-1}\equiv\beta_1{}^{-1}(0)=0.05\text{ F}. \tag{3.18}$$

Several numerical checks using $\beta_0{}^{-1}=0.1$ F and $\beta_0{}^{-1}=0.01$ F showed our results to be completely insensitive to this parameter.

IV. GENERAL RESULTS

Calculations were done for five different values of p_0, the incident kaon lab momenta: 110, 140, 170, 200, and 230 MeV/c. In each of these the N-N potential parameters were those given in Eqs. (3.8) and (3.9). After the

[9] M. A. Melkanoff, D. J. Prowse, D. H. Stork, and H. K. Ticho, Phys. Rev. Letters **5**, 108 (1960).
[10] V. J. Stenger *et al.*, Phys. Rev. **134**, B1111 (1964).

preliminary calculations mentioned above, the K-N isospin triplet parameters were fixed at the values $a_1=-0.29$ F, $\beta_1^{-1}=0.145145$ F, while the K-N isospin singlet-range parameter was kept at $\beta_0^{-1}=0.05$ F. The other K-N $I=0$ parameter was taken to be $a_0=0.04$ F, $a_0=0.08$ F, or $\lambda_0\equiv\lambda_1(0)=0$. The particulars of the methods of analytic continuation, contour integration and matrix inversion used to obtain η_l from Eqs. (2.14)–(2.17) may be found in A.

For each set of input parameters $\eta_l^{\rm IA}$, the impulse-approximation (IA) value for η_l, was calculated from Eq. (2.15) for $l\leqq 9$. The double-scattering (DS) corrections to the IA, $\eta_l^{\rm DS}$, as given by Eq. (2.16) with $R_{l\alpha\beta}$ replaced by $K_{l\alpha\beta}$ were calculated for $l\leqq 3$. The multiple-scattering (MS) corrections to the IA, $\eta_l^{\rm MS}$: (which includes $\eta_l^{\rm DS}$) were calculated for $l=0$, 1, and (at $p_0=230$ MeV/c only) 2. In Table I we show the low l

TABLE I. Values of $\eta_l^{\rm IA}$, $\eta_l^{\rm DS}$, $\eta_l^{\rm MS}$ for $a_0=0.04$ F at the three kaon lab momenta 230, 170, and 110 MeV/c. The entries in the table are in units of 10^{-5} MeV^{-2}.

p_0 (MeV/c)	l	$\eta_l^{\rm IA}$	$\eta_l^{\rm DS}$	$\eta_l^{\rm MS}$
230	0	$2.228-i0.390$	$-0.172\ -i0.074$	$-0.194\ -i0.292$
	1	$0.390-i0.073$	$0.0016+i0.0068$	$0.0016+i0.0053$
	2	$0.081-i0.016$	$0.0003-i0.0002$	$0.0003-i0.0002$
	3	$0.020-i0.004$		
	4	$0.005-i0.001$		
	5	$0.002-i0.000$		
170	0	$2.818-i0.300$	$-0.202\ -i0.066$	$-0.284\ -i0.355$
	1	$0.332-i0.039$	$0.0026-i0.0046$	$0.0024-i0.0034$
	2	$0.049-i0.006$	$0.0001-i0.0002$	
	3	$0.009-i0.001$		
	4	$0.002-i0.000$		
110	0	$3.542-i0.145$	$-0.228\ -i0.037$	$-0.449\ -i0.407$
	1	$0.217-i0.010$	$0.0024-i0.0016$	$0.0021+i0.0008$
	2	$0.018-i0.001$	$-0.0002-i0.0001$	
	3	$0.002-i0.000$		

values obtained for $\eta_l^{\rm IA}$, $\eta_l^{\rm MS}$, and $\eta_l^{\rm DS}$ at $p_0=110$, 170, and 230 MeV/c using $a_0=0.04$ F. It is clear from this table that at each value of p_0 the neglect of all $\eta_l^{\rm IA}$ with $l>9$ and the neglect of all $\eta_l^{\rm DS}$ with $l>3$ are justified. Also it may be seen that for $l>1$ $\eta_l^{\rm MS}$ may be replaced by $\eta_l^{\rm DS}$. Such features of this table as the dominance of the S-wave terms, the slower fall off with l in the values of $\eta_l^{\rm IA}$ at the higher values of p_0, and the relatively larger MS corrections at lower values of p_0 are not unexpected. Perhaps the most interesting point in this table is that although the DS and MS corrections to the real part of $\eta_0^{\rm IA}$ are small ($\lesssim 10\%$), the MS corrections to the imaginary part of $\eta_0^{\rm IA}$ and the differences between the imaginary parts of $\eta_0^{\rm DS}$ and $\eta_0^{\rm MS}$ are very large. This point will be considered in detail in Sec. V.

Having observed the relative sizes of the various η_l given in Table I, we proceeded to calculate the cross sections given in Eqs. (2.11)–(2.13) in the following manner. First, each cross section was calculated in impulse approximation; i.e., for each $l\leqq 9$ we used $\eta_l=\eta_l^{\rm IA}$. Next, each cross section was calculated in a double scattering (DS) approximation; i.e., we used $\eta_l=\eta_l^{\rm IA}+\eta_l^{\rm DS}$ for $l\leqq 3$ and $\eta_l=\eta_l^{\rm IA}$ for $3<l\leqq 9$. Finally

TABLE II. Elastic and total K^+-d cross sections from 110 to 230 MeV/c. The cross sections are given for the impulse approximation (IA) the double-scattering approximation (DS) and the exact multiple-scattering (MS) calculation.

p_0 (MeV/c)	a_0 (F)	$\sigma_{\rm EL}$ (mb) IA	DS	MS	$\sigma_{\rm TOT}$ (mb) IA	DS	MS
110	0.04	24.06	21.10	18.96	6.27	7.40	20.44
140	0.00[a]	21.34	17.99	17.25	8.68	10.55	20.05
	0.04	19.51	17.05	16.16	8.72	9.97	19.16
	0.08	17.79	16.20	15.11	8.92	9.46	18.34
170	0.00[a]	17.37	14.64	14.60	10.32	12.15	18.96
	0.04	15.85	13.86	13.63	10.40	11.60	18.22
	0.08	14.44	13.08	12.69	10.59	11.10	17.60
200	0.00[a]	14.17	12.03	12.34	11.45	13.08	18.10
	0.04	12.97	11.37	11.49	11.52	12.58	17.52
	0.08	11.80	10.71	10.67	11.76	12.19	17.01
230	0.04	10.63	9.38	9.69	12.30	13.24	16.94

[a] The value 0.00 in this column refers to λ_0 rather than a_0.

the full multiple-scattering (MS) calculation for each cross section was performed; i.e. we used $\eta_l=\eta_l^{\rm IA}+\eta_l^{\rm MS}$ for $l\leqq 1$, $\eta_l=\eta_l^{\rm IA}+\eta_l^{\rm DS}$ for $1<l\leqq 3$, and $\eta_l=\eta_l^{\rm IA}$ for $3<l\leqq 9$.

In Table II we list the values obtained for the elastic cross section $\sigma_{\rm EL}$ and the total cross section $\sigma_{\rm TOT}$ in the impulse approximation (IA), the DS approximation, and the MS calculation at five equally spaced values of p_0 from 110 to 230 MeV/c. For $p_0=110$ MeV/c and $p_0=230$ MeV/c the cross sections were calculated using $a_0=0.04$ F, while at the other values of p_0 results were also obtained using $a_0=0.08$ F and using $\lambda_0=0.00$.

From a perusal of Table III we may extract the following information. First, throughout the whole momentum range the IA values are a fair approximation to the MS values of $\sigma_{\rm EL}$. At worst ($p_0=110$ MeV/c) the IA value for $\sigma_{\rm EL}$ is too large by $\approx 25\%$, while at best ($p_0=230$ MeV/c) the IA value for $\sigma_{\rm EL}$ is too large by $\approx 10\%$. Moreover, the DS approximation to $\sigma_{\rm EL}$ is a good approximation in this momentum range giving a result differing by 3–10%. This is an important result in that the DS approximation to $\sigma_{\rm EL}$ is much easier to calculate than the exact answer, there being no integral equation to solve.

For $\sigma_{\rm TOT}$, on the other hand, the IA and DS results are far too small. This is just a reflection of the large values obtained for the imaginary part of each $\eta_0^{\rm MS}$ in Table I. That the IA and DS results for $\sigma_{\rm EL}$ are almost correct reflects the fact shown in Table I that

$$|{\rm Re}(\eta_0^{\rm IA})|\gg|{\rm Im}(\eta_0^{\rm IA})|$$

and

$$|{\rm Re}(\eta_0^{\rm IA}+\eta_0^{\rm DS})|\gg|{\rm Im}(\eta_0^{\rm IA}+\eta_0^{\rm DS})|\,;$$

i.e.,

$$|\eta_0|^2\approx|{\rm Re}(\eta_0)|^2$$

and ${\rm Re}(\eta_0)$ is about right in both these approximations.

The dependence of the IA values for the cross sections

TABLE III. Values of η_0^{IA}, η_0^{DS}, η_0^{MS} at $p_0=170$ MeV/c for various combinations of λ_2, a_0, and a_1. The entries in the table are in units of 10^{-6} MeV^{-2}.

Row number	λ_2	a_0 (F)	a_1 (F)	η_0^{IA}	$\eta_0^{IA}+\eta_0^{DS}$	$\eta_0^{IA}+\eta_0^{MS}$
1.		0.04	−0.29	$28.178-i2.997$	$26.156-i3.652$	$25.340-i6.549$
2.		0.00[a]	−0.29	$29.503-i2.978$	$26.838-i3.958$	$26.174-i6.933$
3.		0.04	0.00[b]	$-1.325-i0.019$	$-1.313-i0.011$	$-1.313-i0.011$
4.		row 2+row 3		$28.178-i2.997$	$25.525-i3.969$	$24.861-i6.944$
5.	0.0	0.04	−0.29	$28.178-i2.997$	$26.156-i3.652$	$26.319-i3.630$
6.	0.0	0.00[a]	−0.29	$29.503-i2.978$	$26.838-i3.958$	$27.172-i3.870$
7.	0.0	0.04	0.00[b]	$-1.325-i0.019$	$-1.313-i0.011$	$-1.313-i0.011$
8.		row 6+row 7				$25.859-i3.881$
9. Chew approximation to row 1: $\eta_0^c=27.127-i4.721$						

[a] The value 0.00 in this column refers to λ_0, not a_0.
[b] The value 0.00 in this column refers to λ_1, not a_1.

on the size of the K-N isospin singlet amplitude shown in Table II is also easily understood. At a given value of p_0 we see that σ_{EL} decreases while σ_{TOT} increases with increasing size of this amplitude. This is merely the result of interference between this amplitude and the triplet amplitude. As a_0 and a_1 have opposite signs and $|a_1|\gg a_0$ the sum of the two scattering amplitudes has a real part that is slightly smaller than the real part of the triplet amplitude by itself while the imaginary part of this sum is slightly larger than that of the triplet amplitude alone. As the DS and MS corrections to σ_{EL} are relatively small this pattern of destructive interference carries over to the DS and MS values for this cross section. This is not so for σ_{TOT} where the MS and DS corrections are large.

We have taken the MS values for σ_{EL} and σ_{TOT} from Table I, and plotted them in Fig. 1 to show graphically their energy dependence and their dependence on the K-N singlet amplitude. It is clear from this figure that the differences in both σ_{EL} and σ_{TOT} due to the variation in the size of the K-N singlet amplitude are quite small. We have also indicated in Fig. 1 by x's the values obtained for the cross sections when the relativistic phase space and the relativistic transformation from laboratory to center-of-mass coordinates are used rather than their nonrelativistic counterparts. These relativistic "corrections" are rather small, being about the same size as the variation due to uncertainty in the size of the K-N singlet amplitude. Although it is not consistent to do so within the framework of our calculation, these relativistic "corrections" should probably be taken into account whenever a direct comparison with experiment is made.

In Fig. 2 we have plotted the MS values for the angular distribution at $p_0=110$, 170, and 230 MeV/c, in which we have used $a_0=0.04$ F. The dashed curves are the same cross sections including the relativistic "corrections" mentioned above. These corrections only get to be significant for small-angle scattering at the higher values of p_0.

In Fig. 3 we have plotted the IA, DS, and MS values for the angular distribution at $p_0=110$ MeV in which we have used $a_0=0.04$ F. The same curves at $p_0=170$ MeV/c and $p_0=230$ MeV/c are shown in Figs. 4 and 5, respectively. Only at $p_0=110$ MeV/c is the DS result not an excellent approximation.

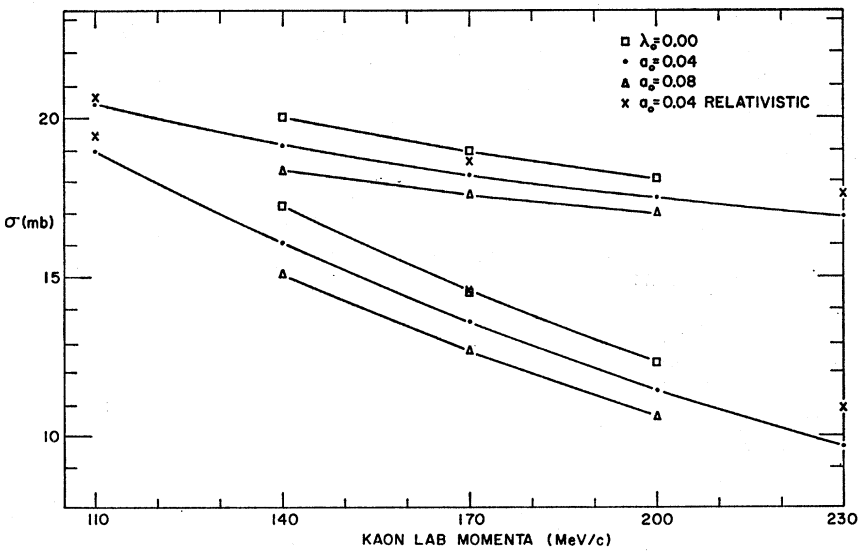

FIG. 1. Total and elastic cross sections as a function of kaon lab momentum for three different values of the isosinglet scattering length. The upper curve of each pair represents the total cross section. The points marked x are for the case $a_0=0.04$ F but with relativistic "corrections."

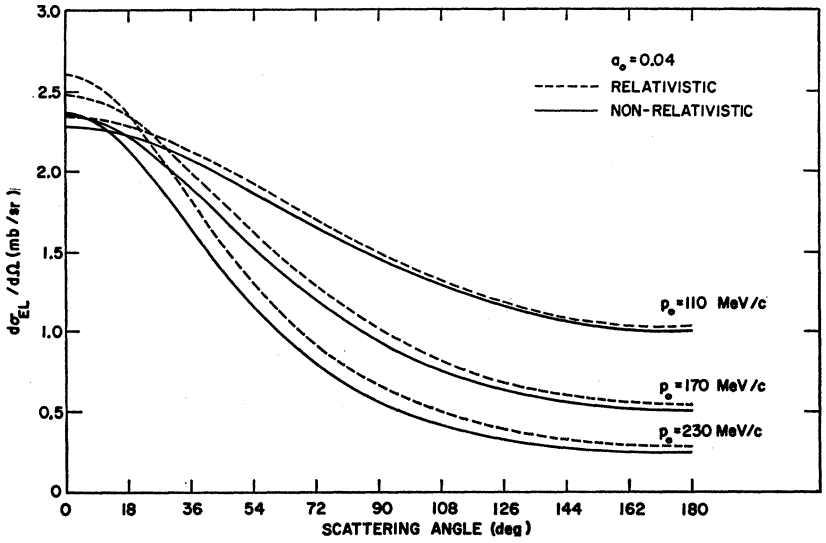

FIG. 2. Differential scattering cross section at various incident lab momentum with and without relativistic "corrections."

The rather small variation of the angular distribution with the size of the K-N singlet amplitude for a typical case is shown in Fig. 6.

V. S-WAVE DETAILS

In order to obtain a better understanding of the S-wave results of Table I some further calculations were performed at $p_0=170$ MeV/c. The results of these calculations (along with some relevant results from Table I) are given in Table III and Fig. 7.

Our first task was to determine which of the higher order MS terms was responsible for the difference $\mathrm{Im}(\eta_0^{\mathrm{DS}}-\eta_0^{\mathrm{MS}})$. This was accomplished by "turning off" various combinations of the three interactions.

From row 7 of Table III it is clear that scatterings which involve only the K-N $I=0$ interaction are of negligible importance. From row 3 it follows that even with the inclusion of intermediate N-N scatterings the terms containing this interaction contribute a negligible amount to η_0. Row 4 gives the contribution to η_0 from all terms which do not include both K-N isotriplet and isosinglet scatterings. Row 2 gives the contribution from all terms which do not contain any K-N isosinglet scatterings. Comparison of these rows with row 1 indicates that any term with a K-N isosinglet scattering in it is small. Rows 5 through 8 indicate that this argument is unchanged when λ_2 is set equal to zero. Since a_0 itself is so small this is to be expected. The difference $\mathrm{Im}(\eta_0^{\mathrm{DS}}-\eta_0^{\mathrm{MS}})$ arises therefore either out of the MS terms that contain only repeated K-N $I=1$ scatterings or out of the MS terms that contain these scatterings and N-N scatterings as well. A comparison of the last column of rows 5 and 1 (or rows 6 and 2) shows that it is the MS terms that contain one or more N-N scatterings that give the overwhelming contribution to $\mathrm{Im}(\eta_0^{\mathrm{DS}}-\eta_0^{\mathrm{MS}})$.

To pinpoint further the terms of interest we evaluated

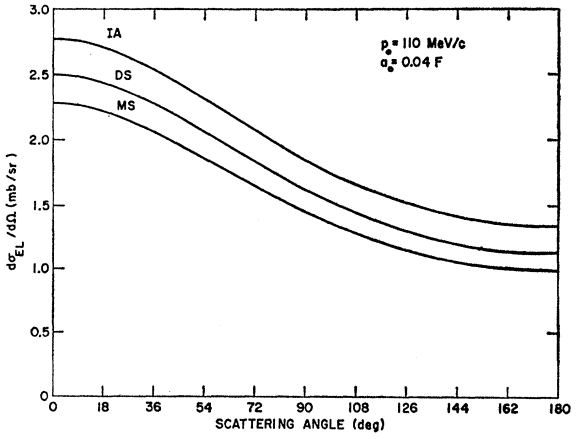

FIG. 3. Differential scattering cross sections at 110-MeV/c kaon lab momentum for the case $a_0=0.04$ F in impulse approximation (IA), double-scattering approximation (DS) and for the full multiple-scattering treatment (MS).

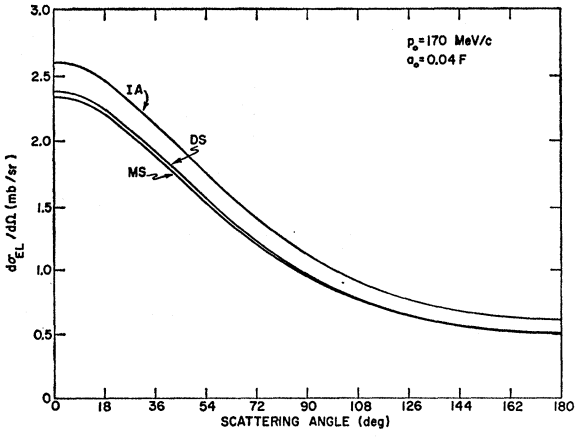

FIG. 4. Differential scattering cross sections at 170-MeV/c kaon lab momentum for the case $a_0=0.04$ F in impulse approximation (IA) double-scattering approximation (DS) and for the full multiple-scattering treatment (MS).

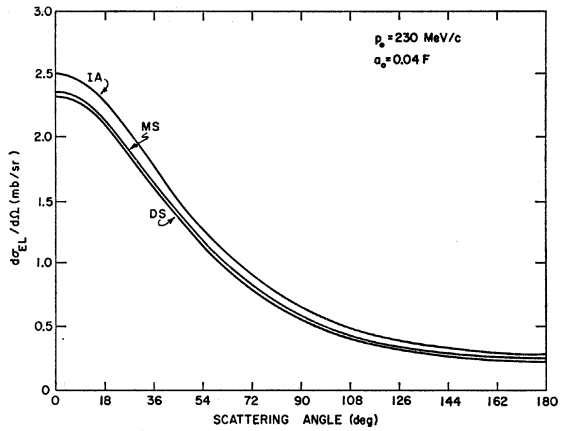

FIG. 5. Differential scattering cross sections at 230-MeV/c kaon lab momentum for the case $a_0=0.04$ F in impulse approximation (IA) double-scattering approximation (DS) and for the full multiple-scattering treatment (MS).

η_0^{MS} by iterating Eq. (2.17) 14 times and at each step using the iterated value of $R_{0\alpha\beta}$ in Eq. (2.16). The results of this calculation are given in Fig. 7. The vector labeled n ($n=1, 2, \cdots, 7$) represents the contribution of all nth-order terms in the MS series for η_0. It is clearly the triple-scattering terms that contribute the bulk of the difference $\mathrm{Im}(\eta_0^{DS}-\eta_0^{MS})$. Combining this result with the conclusions drawn from Table III it is the term

$$\eta_0(121)\equiv\int\Phi_{032}(q,q_a)\tau_1(q,1)K_{032}(q,q'')\times\tau_2(q'',0)K_{023}(q'',q')\tau_1(q',1)\Phi_{032}(q',q_a)\times(qq'q'')^2(2\pi)^{-6}dqdq'dq'', \quad (5.1)$$

which contributes most to this difference.

Qualitatively this result is quite reasonable: The K-N $I=1$ interaction although much larger than the $I=0$ interaction is in the energy range of interest rather small itself; e.g., the phase shift for this interaction at a kaon lab momenta of 175 MeV/c is about $-10°$.[8] Repeated isotriplet scatterings of the kaon from nucleon to nucleon are therefore unlikely and contribute only weakly to η_0. On the other hand, the N-N interaction in the $^3S_1$ state is large. In particular the imaginary part of $\tau_2(q,0)$ contains a δ function corresponding to the deuteron bound state. It is reasonable then to expect $\eta_0(121)$ to be a more important term than $\eta_0(111)$ or even the DS term $\eta_0(11)$.[11]

As for the physics of the situation it may be seen that unitarity indicates $\mathrm{Im}(\eta_0(121))$ should be a sizeable correction to $\mathrm{Im}(\eta_0^{IA})$.[12] Let us denote the t matrices for K-d, K-$N(I=1)$, K-$N(I=0)$, and N-N scattering by T, t_1, t_0, and t_2, respectively, where the t_j are 3-particle operators with the jth particle free. Let us denote the free 3-particle Green's function by G_0 and the Green's function for a free kaon and two interacting nucleons by G_2. Then ignoring the very small t_0, we may with the aid of the identity

$$G_2=G_0+G_0t_2G_0, \quad (5.2)$$

resume the MS series

$$T=t_1+t_1G_0t_1+t_1G_0t_2G_0t_1+\cdots, \quad (5.3)$$

into the form

$$T=t_1+t_1G_2t_1+t_1G_2t_1G_2t_1+\cdots. \quad (5.4)$$

Unitarity demands[13]

$$\mathrm{Im}\langle a|T|a\rangle=-\pi\sum_n\langle a|T|n\rangle\langle n|T^\dagger|a\rangle\delta(E_a-E_n), \quad (5.5)$$

where $|a\rangle$, $|n\rangle$ are eigenfunctions of the asymptotic Hamiltonian (i.e., the Hamiltonian with the K-N interactions turned off) H_2. Ignoring the relatively small $\mathrm{Im}(t_1)$ (e.g., see below or Table I), to lowest order in t_1 we obtain from Eq. (5.4)

$$\mathrm{Re}\langle n|T|m\rangle=\mathrm{Re}\langle n|t_1|m\rangle=\langle n|t_1|m\rangle. \quad (5.6)$$

To lowest order in t_1, Eq. (5.5) then requires

$$\mathrm{Im}\langle a|T|a\rangle=-\pi\sum_n\langle a|t_1|n\rangle\langle n|t_1^\dagger|a\rangle\delta(E_a-E_n). \quad (5.7)$$

But the right-hand side of this last equation may be

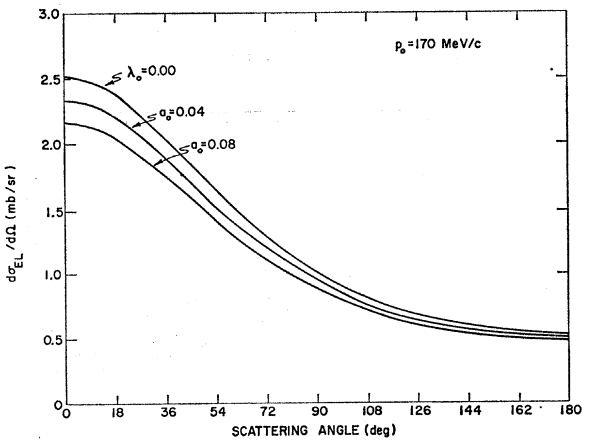

FIG. 6. Differential scattering cross section at kaon lab momentum of 170 MeV/c for the three values of the isosinglet scattering length.

[11] On the same basis, the 5th-order MS terms which include $\eta_0(12121)$ should contribute about as much to η_0 as the 4th-order terms $\eta_0(1211)$ and $\eta_0(1121)$, both being smaller than the third-order contribution. The size of the 6th- and 7th-order terms should also be about the same, both being smaller than the 4th- and 5th-order terms. These relationships are indeed borne out in Fig. 7.

[12] For another approach to unitarity corrections see N. M. Queen, University of Birmingham (unpublished).

[13] B. A. Lippmann and J. Schwinger, Phys. Rev. **79**, 469 (1950).

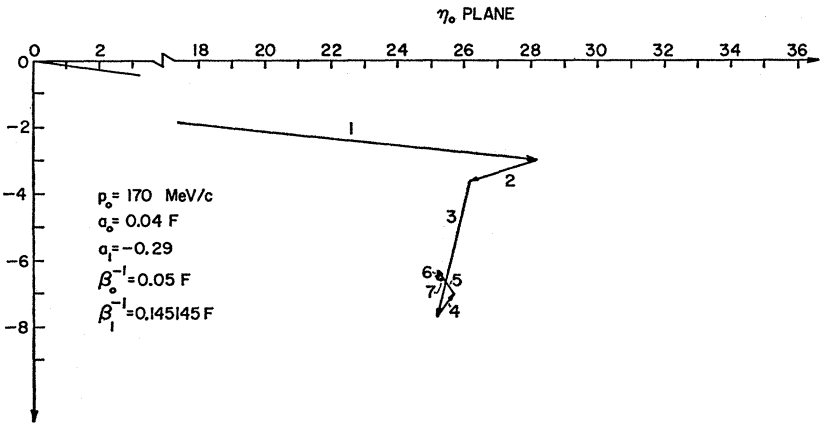

FIG. 7. The complex quantity η_0 for the first seven orders of multiple scattering. Arrows labeled 1, 2, etc., represent contributions from single, double, etc., scatterings, respectively. The units of η_0 are 10^{-6} MeV^{-2}.

written

$$-\pi\sum_{n,m}\langle a|t_1|m\rangle\langle m|\delta(E_a-H_2)|n\rangle\langle n|t_1|a\rangle$$
$$=-\pi\langle a|t_1\delta(E_a-H_2)t_1|a\rangle$$
$$=\mathrm{Im}\langle a|t_1G_2t_1|a\rangle. \quad (5.8)$$

To satisfy unitarity to lowest order we must keep the contribution of $t_1G_2t_1$ to the imaginary part of the scattering amplitude. From Eq. (5.2) this term contains both $\eta_0(11)$ and $\eta_0(121)$. In other words, with neither η_0^{IA} nor with $\eta_0^{\mathrm{IA}}+\eta_0^{\mathrm{DS}}$ may unitarity be satisfied to lowest order in t_1, but $\eta_0^{\mathrm{IA}}+\eta_0^{\mathrm{DS}}+\eta_0(121)$ does satisfy unitary to this order. We would expect $\mathrm{Im}(\eta_0^{\mathrm{IA}})$ to be too small, $\mathrm{Im}(\eta_0^{\mathrm{IA}}+\eta_1^{\mathrm{DS}})$ to be not much larger, and $|\mathrm{Im}(\eta_0^{\mathrm{MS}})|\approx|\mathrm{Im}(\eta_0(121))|\gg|\mathrm{Im}(\eta_0^{\mathrm{DS}})|$.[14] This is indeed the case.[15]

The last type of approximation that we investigated was the "Chew approximation."[16] Here $\eta_0(\equiv\eta_0^c)$ is calculated using just the single-scattering terms, but the K-N amplitudes are taken outside the average over the deuteron momentum distribution and evaluated as on-energy-shell t-matrix elements, the energy of the K-N relative motion being determined by $k=(\mu_{KN}/\mu_{Kd})q_a$. The results for η_0^c in this approximation are given in row 9 of Table III; i.e., $\mathrm{Re}(\eta_0^c)\approx\mathrm{Re}(\eta_0^{\mathrm{IA}})$ while $|\mathrm{Im}(\eta_0^c)|>|\mathrm{Im}(\eta_0^{\mathrm{IA}})|$. These results may be understood on the basis of the following qualitative analysis.

We again ignore the K-N $I=0$ interaction. From Eq. (2.5) and our work in Sec. III it follows that

$$\tau_1(q)=\frac{2\pi(\beta_1^2+k^2)^2}{\mu_1}\left[\frac{2\pi(\beta_1^2+k^2)^2}{\mu_1\lambda_1}+\frac{(\beta_1+ik)^2}{2\beta_1}\right]^{-1}, \quad (5.9)$$

where k is given in terms of q_a by Eq. (3.2). We have taken λ_1 to be so large that Eq. (5.9) may be well approximated by

$$\tau_1(q)=4\pi\beta_1(\beta_1-ik)^2\mu_1^{-1}. \quad (5.10)$$

Again using Eq. (3.2) we see that

$$\mathrm{Re}(\tau_1(q))=\frac{4\pi\beta_1}{\mu_1}\begin{cases}(\beta_1^2-k^2), & q\leq q_0\\ (\beta_1-ik)^2. & q>q_0\end{cases}, \quad (5.11)$$

$$\mathrm{Im}(\tau_1(q))=\frac{4\pi\beta_1}{\mu_1}\begin{cases}-2\beta_1k, & q\leq q_0\\ 0, & q>q_0\end{cases}, \quad (5.12)$$

where

$$q_0=[2m_1\mathfrak{M}_1\mathfrak{M}^{-1}E]^{1/2}. \quad (5.13)$$

Because of the peaking of $\Phi_{032}(q,q_a)$ the only values of k for which contributions to the integrand of Eq. (2.15) with $l=0$ are significant are those for which $|k|\ll\beta_1$. Thus

$$\mathrm{Re}(\tau_1(q))\approx4\pi\mu_1^{-1}\beta_1^3. \quad (5.14)$$

Within this approximation $\mathrm{Re}(\tau_1(q))$ is a constant which may be taken outside of the integral over q; i.e., $\mathrm{Re}(\eta_0^{\mathrm{IA}})\approx\mathrm{Re}(\eta_0^c)$.

For $\mathrm{Im}(\tau_1(q))$ the situation is quite different. From Eqs. (5.12) and (3.2) $\mathrm{Im}(\tau_1(q))$ is a monotonically increasing function of q for $0\leq q\leq q_0$ and vanishes for $q=q_0$. Furthermore, from Eq. (5.13) $\mathrm{Im}(\tau_1(q))$ vanishes in the middle of the range of q's that contribute significantly to the integral in Eq. (2.15); i.e., ignoring the deuteron binding energy $q_0\approx1.2q_a$. On the other hand, in the Chew approximation, $\mathrm{Im}(\tau_1(q))$ is evaluated at $q=q_a/2$, a value of q so small that $|\mathrm{Im}(\tau_1(q))|$ is close to its maximum value. It necessarily follows that $|\mathrm{Im}(\eta_0^c)|>|\mathrm{Im}(\eta_0^{\mathrm{IA}})|$.

Calculations of the elastic angular distribution and elastic cross section that included all partial waves were carried out using the Chew approximation with p_0 in the range 110–230 MeV/c. In all cases the results were somewhat better than the IA results discussed above and at the lower values of p_0 the results were as good as those obtained with the DS approximation. The Chew

[14] $\mathrm{Re}(\eta_0(121))$ may well be about the same size as $\mathrm{Im}(\eta_0(121))$, but since $\mathrm{Re}(\eta_0^{\mathrm{IA}})\gg|\mathrm{Im}(\eta_0^{\mathrm{IA}})|$ it would be a relatively small correction.

[15] This argument must be modified if $\mathrm{Im}\langle a|t_1|a\rangle$ is large as in K^--d scattering where the $\bar{K}$-N amplitude has a large absorptive part.

[16] G. F. Chew, Phys. Rev. **80**, 196 (1950); G. F. Chew and G. C. Wick, *ibid.* **85**, 636 (1952); G. F. Chew and M. L. Goldberger, *ibid.* **87**, 778 (1952).

approximation for elastic K^+-d scattering therefore is both more accurate and easier to calculate than the IA and for the range of p_0 considered here it is a good approximation.

VI. SUMMARY

We have performed a multiple-scattering analysis of low-energy K^+-d elastic scattering. We assumed that all two-body interactions were separable S-wave potentials of the Yamaguchi form. The parameters in these potentials were chosen so as to be in agreement with available low-energy data. Coulomb forces and the K^+-K^0 and n-p mass differences were neglected.

Results were presented for the elastic angular distribution, elastic cross section, and total cross section for incident kaon lab momenta p_0 of 110, 140, 170, 200, and 230 MeV/c. The meat of these results may be stated as follows:

(i) The values obtained for the cross sections were insensitive to the values of the parameters used in the very small K-N isosinglet interaction.

(ii) Throughout the energy range discussed the elastic angular distribution and cross section could be well approximated by the low-order terms in the multiple-scattering series. The single-scattering terms alone (with the K-N amplitudes either inside or outside the average over the deuteron momentum distribution) gave a value for σ_{EL} that at worst (i.e., at $p_0=110$ MeV/c) was too large by $\approx 25\%$. Inclusion of the double-scattering terms reduced this difference to 10% or less. These results could be explained qualitatively on the basis of the rather small K-N isotriplet interaction and the dominance of elastic over inelastic scattering in the energy range being considered.

(iii) With only single- and double-scattering terms a reasonable (within 25% of the correct value) approximation to σ_{TOT} was obtained only for $p_0=230$ MeV/c. To obtain an approximation for σ_{TOT} valid throughout the range $110 \leqq p_0 \leqq 230$ it was necessary to include at least the third-order multiple-scattering term that contained an intermediate nucleon-nucleon scattering. This result agreed qualitatively with arguments based on unitarity.

ACKNOWLEDGMENTS

We wish to express our appreciation to Lawrence Liddiard and the rest of the staff of the University of Minnesota Numerical Analysis Center for their help and cooperation.